The Project evalAT for Investigating the Accuracy of Aerotriangulations in Map Projections

Camillo Ressl[1], Norbert Pfeifer[1], Christine Ressl[2], Andreas Bayr[2]

[1] TU Wien, Department of Geodesy and Geoinformation, Research Unit Photogrammetry, Wiedner Hauptstraße 8-10, 1040 Wien - [Camillo.Ressl, Norbert.Pfeifer]@tuwien.ac.at
[2] BEV – Federal Office of Metrology and Surveying, Department G2 – Remote Sensing, Schiffamtsgasse 1-3, 1020 Wien - [Christine.Ressl, Andreas.Bayr]@bev.gv.at

Keywords: aerotriangulation, accuracy, map projection, adjustment.

Abstract

This paper investigates the accuracy of the aerial triangulation (AT) performed in a conformal map projection for a GNSS-INS-supported image block consisting of 4342 vertical images, GSD 20 cm, with 22 main strips and 5 cross strips. Using 169 check points the obtained results are compared with the accuracy achieved by running the AT in an undistorted tangential system. It turns out, that in both systems the same accuracies can be achieved, with RMSE in (X, Y, Z) of (7, 10, 11) cm, if Earth curvature and scale distortion are correctly modelled in the map projection. If the scale distortion is not considered, then the RMSE in Z increases by 100% to 300% (depending on the height distribution of the GCPs). In AT software packages that do not consider the scale distortion a partial compensation is possible by either adapting the height of the projection centres or the principal distance leading to RMSE of around (10, 11, 15) cm.

1. Introduction

One task of the Austrian mapping agency (BEV) is the topographic survey of the national territory by means of aerial images (BEV, 2025a). The resulting photogrammetric products, mainly orthophoto mosaics and elevation models derived by image matching, are to be provided in the map projection of the Austrian national system (MGI). The aerial triangulation (AT), necessary to generate these products, is therefore also executed in this map projection.

The MGI system uses the Bessel 1841 ellipsoid and was established in the 19th century. The national *MGI heights* (German *Gebrauchshöhen*) are normal-orthometric heights referenced to the Adriatic Sea level. The Austrian map projection is the conformal Gauss-Krüger projection. Because of historically induced distortions in the MGI system, any 3D results derived from current observations require a subsequent location-based adaptation to be in line with this official system: The X and Y coordinates are modified by the so-called *GIS-Grid* (BEV, 2025b) and the Z coordinates by the so-called *Height-Grid* (BEV, 2025c).

Occasionally, the elevation models derived from recent aerial images showed unexpected large differences to other elevation data (particularly in alpine regions). An obvious cause for these observed errors could be the mentioned irregular adaptations in X, Y, Z in the map and shortcomings when establishing the collinear relation between image and object point in the map projection.

Therefore, the BEV initiated the project evalAT[1] in cooperation with TU Wien in order to determine the cause of the observed height errors and to generally evaluate the accuracy potential of aerial triangulations done in the map projection. Thereby, the AT accuracy in the map projection is determined using independent check points and compared with the accuracy obtained in an undistorted system. For the latter, a 3D system is used, which has its XY plane tangential to the reference ellipsoid in the centre of the block of images (termed *tangential system*).

2. Theoretical Background on Photogrammetry in Conformal Map Projections

Applying the collinearity equation for aerial images requires the consideration of the (physically caused) refraction (McGlone, 2013, p. 340). For photogrammetric computations in a (conformal) map projection additionally the (geometrically caused) earth curvature (EC) needs to be considered (Wang, 1980, p. 64). The necessity for both corrections is known basically since the beginning of photogrammetry. During a test on integrated sensor orientation (Heipke et al, 2002) lead by the EuroSDR (then OEEPE) in 1999, the community became aware that the (also geometrically caused) scale distortion needs to be considered in the map projection also (Ressl, 2002), (Jacobson, 2002).

Based on Figure 1, adapted from (Ressl, 2002), the problem of photogrammetry in a map projection can be described as follows: Sketch (A) shows a vertical section through three selected projection centers of a strip flown along a circle of latitude from west to east. The aircraft flies at a constant ellipsoidal height H_F. The principal distance is c, the image format is s, and the photographs are exactly vertical. If the ellipsoidal area covered by these images is subjected to the Gauss-Krüger projection, the known EC (sketch B) corrects the curvature difference during the transition from the ellipsoid to the plane of the map projection.

[1] A German contribution about this project (Ressl et al., 2025) was presented at the Dreiländertagung 2025 in Muttenz, which forms the base of the present paper.

This contribution has been peer-reviewed. The double-blind peer-review was conducted on the basis of the full paper.
https://doi.org/10.5194/isprs-annals-XI-2-2026-29-2026

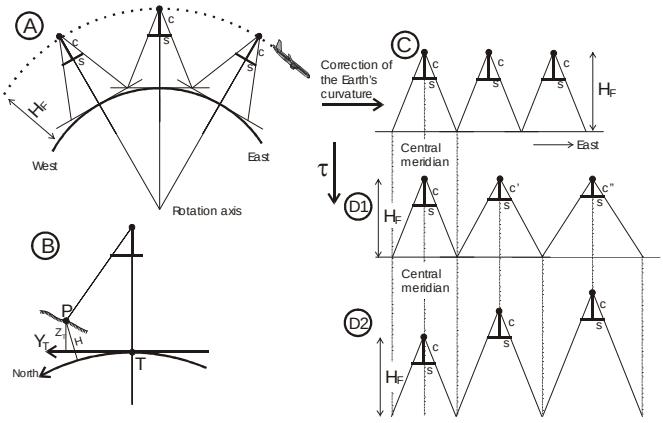

Figure 1. A flight strip and its appearance in the national map taken from (Ressl, 2002). Sketch (A) shows the real situation: absolute (ellipsoidal) flying height H_F, principal distance c, image width s. Sketch (B) depicts the Earth curvature correction in the software Orient. Sketch (C) shows the situation in the map after considering EC. Sketch (D1) and (D2) indicate the subsequent effect that the scale distortion τ has on either the principal distance or the flying height in the map projection.

Now, the “unwrapped” flight strip (sketch C) gets effected by the scale distortion τ, which increases towards east and west from the central meridian of the Gauss-Krüger projection (Snyder, 1987, p. 61). Whereas the XY coordinates in the national coordinate system are derived from the map projection, the ellipsoidal heights are transferred unchanged into the national system as Z-coordinates. Thus, the aircraft now “flies” horizontally at a constant height H_F above the map projection plane. This results in a horizontal-vertical scale difference (i.e., an affinity) that itself changes due to the variable scale distortion.

A discrepancy thus arises, as illustrated in sketches (D1) and (D2): On the one hand, the heights of the projection centers of the images should be equal, since the flight was conducted at a constant ellipsoidal height. However, this would require the image angles to continuously increase eastward due to τ and its increase, meaning the ratio between the principal distance c and the image format s would have to change (sketch D1). On the other hand, if this ratio remains constant (since all images were taken with the same camera), the flight altitude in the national coordinate system would have to continuously increase eastward (sketch D2).

In summary, three problems arise when applying photogrammetry in the national conformal map projection:
P1) The effect of Earth’s curvature
P2) The horizontal-vertical affinity
P3) Continuous variation of the horizontal scale in east-west direction within the block area

While problem P1 is eliminated by Earth curvature correction in most software solutions, problems P2 and P3 are not addressed in every software package. This has led to the publication of ad hoc solutions that consider the scale distortion either in the principal distance of the images (sketch D1) or in the height of the projection centers (sketch D2); (Ressl, 2002), (Legat, 2006). The first method requires vertical images, while the second additionally requires horizontal terrain.

In the TU Wien inhouse software Orient (Kager, 1989), which is primarily used for this study, the EC is implemented per image such that the collinearity equation is formulated in a tangential system centered at the local nadir point of each image (analogous to sketch B). Thereby using the tangential height Z_T, which is derived from the ellipsoidal height H of the object point P in the national system. During the mentioned OEEPE test, this tangential system was extended to include the horizontal-vertical affinity caused by τ. Both corrections (EC and τ) are thus formulated in object space and are essentially independent of terrain shape and image viewing direction.

As mentioned above, the Austrian national surveying system is based on the Gauss-Krüger projection with additional adaptations: After the Gauss-Krüger projection the horizontal coordinates are adapted by location-dependent shifts provided by the so-called *GIS-Grid*, in order to adapt to historically conditioned network tensions (BEV, 2025b). Additionally, instead of the geometrically more correct *ellipsoidal heights*, so-called *MGI heights* are used, which are an approximation to *orthometric heights* and are derived from ellipsoidal heights by applying the geoid and the so-called *Height-Grid* (BEV, 2025c).

3. Data

The study uses a selection of images from the official flight block “2022260_Zeltweg”, which covers an alpine area with terrain elevations ranging from 502 m to 2170 m. Table 1 lists the key parameters, Figure 2 locates the covered area within Austria, and Figure 3 shows the distribution of the flight strips in detail.

The following data were available (provided as part of the operational delivery by the flight contractor originally commissioned by BEV): GNSS-INS trajectory referenced to ETRS89 (geocentric) and the Austrian national system MGI (as Gauss-Krüger projection in the M31 meridian strip system), as well as metadata descriptions (flight mission, calibration protocol, etc.) and the AT project file (in meridian M31 system) of the Inpho Match AT software.

Area	Zeltweg
Size [km]	85 × 41
GSD [cm]	20
Flight dates	7.2022 - 10.2022
# Flight missions	10
Camera	UltraCam-Eagle-M3
Focal length [mm]	100.5
Pixel size [µm]	4.000
Sensor size [pixel]	26460 × 17004
Base [m]	480
Strip separation [m]	1860
Forward / side overlap (valley, 502 m)	84%/61%
Forward / side overlap (top, 2170 m)	76%/40%
# Main-strips (*)	22
# Cross-strips (*)	5
# Images	4342
Trajectory	GNSS & INS

Table 1. Parameters defining the test block of vertical images. (*) The strip count is approximate, because flying some strips in their full E-W or N-S extent took several days; see Fig. 3.

This contribution has been peer-reviewed. The double-blind peer-review was conducted on the basis of the full paper.
https://doi.org/10.5194/isprs-annals-XI-2-2026-29-2026 | © Author(s) 2026. CC BY 4.0 License.

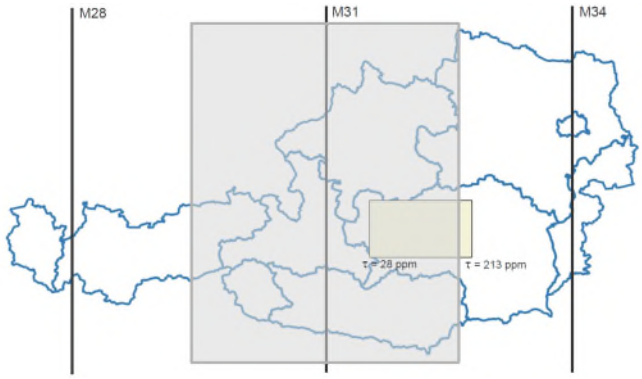

Figure 2. Test block, with east-west extent of 85 km, inside Austria, where the area covered by Gauss-Krüger meridian strip M31 is highlighted in grey. At the western and eastern border of the flight block the scale distortion is 28 ppm and 213 ppm.

For this study, the BEV surveyed 179 terrain points using GNSS within the elevation ranging from 586 m to 2003 m, which serve as control and check points. Of these points, 98 were measured twice, yielding RMS values for the differences in (X, Y, Z) of (2.2, 1.6, 2.3) [cm]. Since the trajectory was recorded using GNSS and INS during the flight, the need for ground control points (GCPs) is limited. Therefore, the smallest meaningful subset of these 179 points was selected as GCPs; specifically, two control points in each corner of the block (see Figure 3). The terrain elevations in these four areas are: 786 m, 617 m, 578 m, and 1257 m. In anticipation of the expected height issues, additionally two control points were included in a particularly high-elevation area within the block (1754 m), thus totalling the number of GCPs to ten.

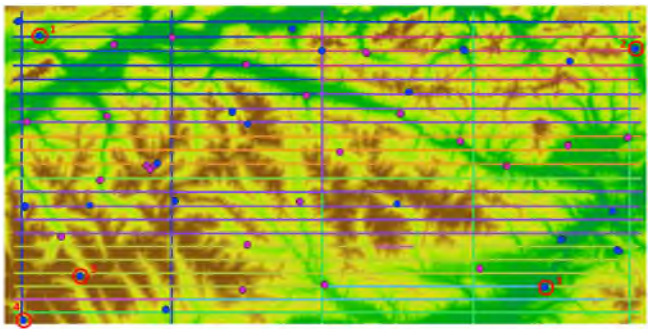

Figure 3. Distribution of the strips inside the block. Each flight mission is shown in a different color. The areas, where BEV measured terrain points by GNSS, are shown in blue (single RTK) and violet (repeated RTK). Per area at least four points were measured. The five areas, where two points were selected as control points, are in red. The heights in these five areas are: 1: 913 m, 2: 762 m, 3: 603 m, 4: 1341 m, 5: 1787 m. The east-west extent is 85 km. Background: color-coded terrain model with legend: 586 m 2003 m.

4. Remarks on the computed Aerial Triangulations

The aim of this study is to determine the potential accuracy of aerial triangulation (AT) in the national map projection. This is assessed using the residuals at the check points. The reference accuracy is determined by performing the AT in an undistorted tangential system.

4.1 Computation Systems

For the transformation into the Austrian national coordinate system, the already distorted coordinates (originating from the original Gauss-Krüger projection) are further distorted using the *GIS-Grid* for the horizontal coordinates and the *Height-Grid*. Both is expected to result in an additional reduction in accuracy. The extent of this accuracy reduction is revealed by comparison with the accuracy in the tangential system. To assess the effects of all these distortions on accuracy, ATs are performed in various coordinate systems using the Orient software (see Table 2).

All GNSS terrain points and the trajectory data are transformed from ETRS to MGI using the Austrian-wide standard transformation (BEV 2025d). The AT in the tangential system represents the geometrically most correct variant, as (apart from refraction) no further distortions need to be considered. In this tangential system the measurement accuracies were verified using variance component estimation (see Table 3) and the choice of additional parameters was decided (see Section 5.1).

Abbr.	System	Remark	
TangSys	ETRS89, GRS80	base point (14.508°, 47.304°, 0 m)	
GK0	MGI, M31, Bessel	no *GIS-Grid*	ellipsoidal heights
GK1			orthometric heights
GK2			MGI heights
GK3		with *GIS-Grid*	MGI heights

Table 2. Overview of the used computation systems.

Among the variants of the Gauss-Krüger projection, the GK0 variant is the geometrically most correct, since the horizontal coordinates are not further adapted to existing network tensions in the official national coordinate system by applying the *GIS-Grid* (Figure 4), and the heights are referenced to the ellipsoid. The GK1 and GK2 variants successively distort the heights by applying the geoid (for orthometric heights) and the *Height-Grid* (for MGI heights; Figure 5), respectively. Finally, the GK3 variant also uses the *GIS-Grid*, thus performing the AT in the official system of the Austrian national survey.

4.2 Weights of the Observations

Each AT uses the observations listed in Table 3 with the accuracies specified there (for weighting). These accuracies were verified in the AT performed in the tangential system using variance component estimation.

Image points	0.2 [pix]
GNSS (proj. centres (X, Y, Z))	(5, 5, 5) [cm]
INS (angles (ω, ϕ, κ))	(1, 1, 5) [mgon]
Ground control points	(5, 5, 5) [cm]

Table 3. Used observations and their accuracies.

This contribution has been peer-reviewed. The double-blind peer-review was conducted on the basis of the full paper.
https://doi.org/10.5194/isprs-annals-XI-2-2026-29-2026 | © Author(s) 2026. CC BY 4.0 License.

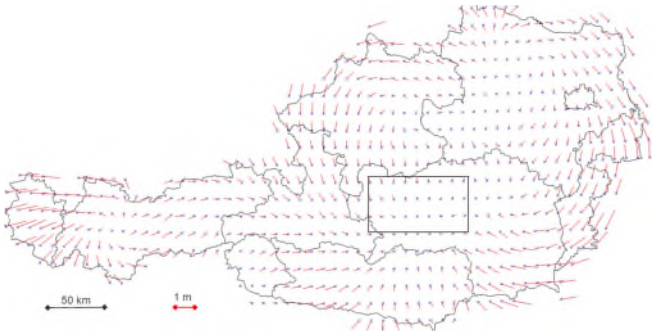

Figure 4. *GIS-Grid* in Austria for transforming the X and Y coordinates from the original Gauss-Krüger projection into the official Austrian system, which contains historically induced distortions (overlayed with the test block boundary).

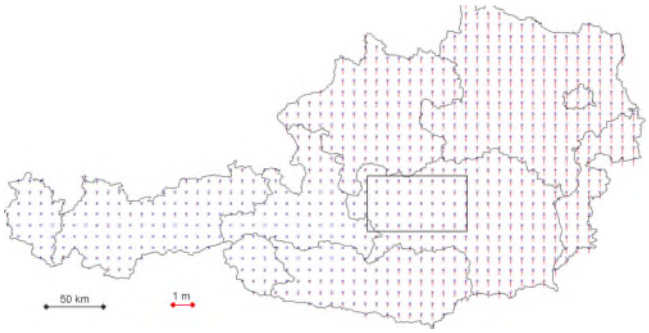

Figure 5. *Height-Grid* in Austria for transforming from orthometric to national MGI heights (overlayed with the test block boundary).

5. Results

The Orient software from TU Wien allows the following corrections to be applied: refraction, Earth curvature, and scale distortion (τ). The latter two are particularly important when performing aerial triangulation (AT) in a map projection.

The image measurements of the tie points were directly adopted from the delivered project file of the Inpho Match-AT software, which usually extracts tie points based on a combination of feature-based and least-squares matching. Due to memory limitations in the Orient software, the number of tie points (originally 228000 object points) had to be reduced. This was done by dividing each image into a 3×3 grid, and then selecting the tie point with the highest multiplicity in each cell. Any selected tie point gets activated in all its containing images, according to its multiplicity. As a result, each image contains significantly more than 9 active tie points (resulting in the end in 7000 object points).

In addition to these automatic tie points, the images also include manual measurements of the ground control and check points. On average, each image contains 22 (control, check or tie) points (minimum 10, maximum 45).

5.1 Tangential System

Systematic offsets between the direct georeferencing measurements (GNSS and INS) and the estimated values are not uncommon. The following causes are often responsible: slight differences in the datum realization of GNSS or changes in the mounting of the sensors in the aircraft. These changes can be constant for the entire flight block or, more frequently, vary slightly across the flight missions (e.g., after removal or reinstallation of sensors or mechanical stress from takeoffs and landings).

One way to compensate for these changes during aerial triangulation is to estimate a 3D shift for the GNSS measurements (either in the platform system (lever arm) or in the global system) and a small corrective rotation for the INS-derived rotations (misalignment). These offsets for GNSS and INS are often collectively referred to as *mounting calibration parameters*. This calibration can be applied jointly for all images of the block or for each flight mission, or grouped for all images of each strip (the latter only makes sense if cross-strips are available).

Figure 6 shows the GNSS residuals after determining a single common 3D shift (and misalignment) for all images of the block in the AT (*block mounting*). Figure 7 shows the GNSS residuals after determining a common 3D shift (and misalignment) for the images of each strip (*strip mounting*). The block variant exhibits clear systematic patterns for individual strips. A comparison with Figure 3 reveals that these patterns partially align very well with the different flight missions. In the strip mounting variant, this systematic pattern disappears.

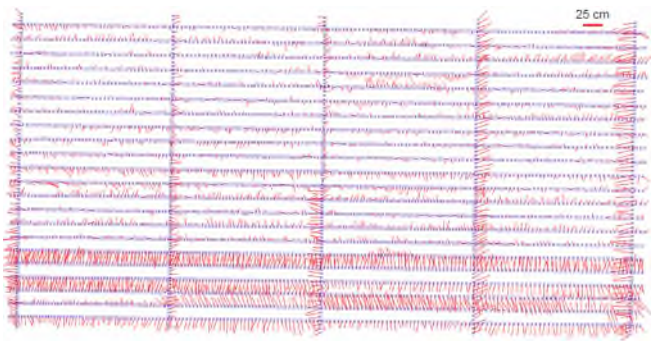

Figure 6. GNSS residuals after estimating a single mounting for the entire block.

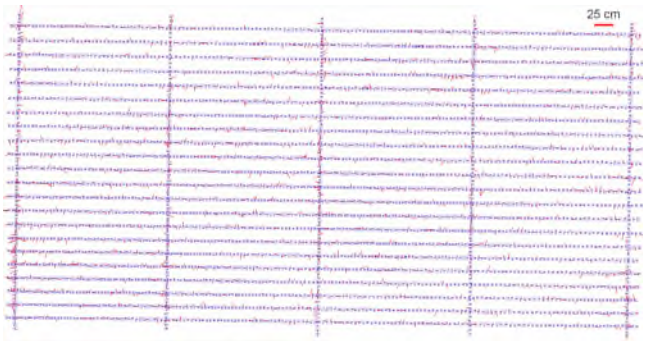

Figure 7. GNSS residuals after estimating a mounting for each strip.

The variance component estimation for these two variants returns estimated accuracies for the direct georeferencing observations of [cm resp. mgon]: GNSS (block: 9, 12, 10; strips: 4, 4, 4) and INS (block: 3, 3, 11; strips: 1, 1, 5). Since the strip-wise mounting approach clearly represents the better of the two models, it is used in all variants.

Table 4 shows the residuals of the ground control and check points. For the variant with strip mountings and 10 GCPs, the XY residuals of the checkpoints are better than 10 cm (roughly half a GSD). In comparison to the 0.2 pix image residuals (in Table 3), the photogrammetric potential appears not to be fully exploited by a factor 2.

This contribution has been peer-reviewed. The double-blind peer-review was conducted on the basis of the full paper.
https://doi.org/10.5194/isprs-annals-XI-2-2026-29-2026 | © Author(s) 2026. CC BY 4.0 License.

[cm]		GCPs (n=10)					check points (n=169)				
		min	mean	medi	MAX	**RMS**	min	mean	medi	MAX	**RMS**
block mount	X	-1	12	13	22	**15**	-10	6	5	33	**10**
	Y	-8	2	3	16	**7**	-21	8	9	29	**12**
	Z	-12	0	1	18	**10**	-45	2	2	40	**14**
strip mount	X	-9	0	2	8	**6**	-14	2	3	16	**7**
	Y	-12	0	-1	12	**7**	-21	3	3	28	**10**
	Z	-10	0	-1	11	**6**	-35	1	2	34	**11**

Table 4. Residuals in [cm] of the terrain points after the AT in the tangential system using 10 GCPs and block or strip mountings.

The check point residuals for the block mounting variant are only slightly worse (by about 3 cm in RMS). This is partly because only a small portion of the strips are affected by the significantly altered mountings. Additionally, to a high degree the large GNSS corrections in Figure 5 compensate for this modelling error (i.e., block vs. strip mounting). Consequently, the numerous tie points are distorted only slightly.

During the investigations in the tangential system, it was found that the interior orientation can be kept constant according to the calibration protocol.

5.2 Gauss-Krüger Projection with Ellipsoidal Heights

To correctly perform an AT in the Gauss-Krüger projection, corrections for refraction, Earth curvature (EC), and scale distortion (τ) must be applied. Table 5 (row “Ref+EC+Tau”) shows the resulting residual statistics of the check points. A comparison with the corresponding variant in the tangential system (Table 4, row “strip mount”) shows, that the residual statistics for the terrain points are effectively identical.

To demonstrate the importance of these three corrections, Table 5 also includes the residuals obtained in case one of the corrections (refraction, Earth curvature, or scale distortion) is omitted. Compared to the correct state with all three corrections, the Z-RMS of the check points deteriorates by 1 cm if refraction is neglected, by 17 cm if Earth curvature (EC) is neglected, and by 12 cm if scale distortion (τ) is neglected.

The ratio of the impact of all three corrections is therefore: Refraction : τ : EC = 1 : 12 : 17. With respect to the two projection-related corrections, the ratio is: τ : EC ≈ 2 : 3.

[cm]		GCPs (n=10)					check points (n=169)				
		min	mean	medi	MAX	**RMS**	min	mean	medi	MAX	**RMS**
Ref EC Tau	X	-9	0	2	8	**5**	-15	2	2	16	**6**
	Y	-13	0	-1	11	**7**	-21	3	3	30	**10**
	Z	-8	0	0	6	**4**	-38	1	0	41	**11**
no Ref	X	-9	0	2	9	**6**	-15	2	2	16	**6**
	Y	-15	0	0	12	**8**	-20	3	3	31	**11**
	Z	-7	0	0	9	**4**	-37	0	-2	43	**12**
no EC	X	-9	0	1	8	**6**	-16	3	4	18	**7**
	Y	-18	0	2	23	**12**	-28	-1	0	36	**10**
	Z	-17	0	-9	40	**20**	-46	4	-2	63	**28**
no Tau	X	-9	0	3	5	**5**	-14	3	4	17	**7**
	Y	-11	0	-3	13	**8**	-20	4	4	32	**11**
	Z	-31	0	11	25	**21**	-51	6	10	44	**23**

Table 5. Residuals of the terrain points after the AT in GK with ellipsoidal heights by considering all corrections (Ref + EC + Tau) and by neglecting one of them. Ref = refraction, EC = Earth curvature, Tau = scale distortion.

5.3 Comparison of all Gauss-Krüger Variants

Table 6 shows the residuals of the terrain points for all examined Gauss-Krüger variants. It is evident that all variants yield practically equivalent check point residuals if all three corrections (refraction, Earth curvature, and scale distortion) are applied. This holds true specifically for the GK3 variant, where the *GIS-Grid* is used and calculations are performed in *MGI heights*.

[cm]		GCPs (n=10)					check points (n=169)				
		min	mean	medi	MAX	**RMS**	min	mean	medi	MAX	**RMS**
GK0: ellip.H	X	-9	0	2	8	**5**	-15	2	2	16	**6**
	Y	-13	0	-1	11	**7**	-21	3	3	30	**10**
	Z	-8	0	0	6	**4**	-38	1	0	41	**11**
GK1: orth.H	X	-8	0	0	11	**6**	-17	2	2	18	**7**
	Y	-12	0	-1	12	**8**	-22	4	4	33	**12**
	Z	-7	0	1	5	**4**	-34	1	1	39	**11**
GK2: prac.H	X	-8	0	0	11	**6**	-18	2	2	18	**7**
	Y	-12	0	-1	12	**8**	-22	4	4	34	**12**
	Z	-7	0	1	5	**4**	-32	1	1	39	**11**
GK3: GISgrid +prac.H	X	-11	0	-2	19	**10**	-25	2	2	22	**8**
	Y	-14	0	0	13	**9**	-21	3	2	29	**11**
	Z	-8	0	1	5	**4**	-34	1	1	39	**11**

Table 6. Residuals in [cm] of the terrain points after the AT in the different GK variants; cf. Table 2.

5.4 Gauss-Krüger Projection without Scale Distortion

Section 5.2 showed that the effect of scale distortion (τ) accounts for approximately two-thirds of the impact of Earth curvature in this dataset. Since the scale distortion is not considered in every commercial software package, Table 7 presents the residuals at the terrain points obtained using the Orient software when scale distortion is intentionally neglected. This analysis is done in the GK3 system, as this system is of particular interest to the BEV (i.e., using *GIS-Grid* and *MGI heights*).

The best variant without considering scale distortion is “GK3: SM” in Table 7 (with strip mountings), which yields a Z-RMS of 23 cm. For comparison: The reference solution (with scale distortion) has a Z-RMS of 11 cm (GK3, with strip mountings; last row in Table 6).

If the GNSS projection centres would be used without any shift in the AT, the Z-RMS even reaches 40 cm (row “GK3: nM” in Table 7). In comparison, the negative effect of neglected scale distortion can be partially mitigated by an unknown block mounting (Z-RMS = 26 cm, row “GK3: BM” in Table 7). This again (similar to the tangential system (Table 4)) is approximately 3 cm larger than the variant with shifts per strip (Z-RMS = 23 cm, row “GK3: SM” in Table 7).

However, the extent to which the effect of scale distortion can be compensated by unknown block or strip mountings also depends on the elevation distribution of the GCPs. If, instead of the previously well-distributed 10 GCPs, 7 GCPs at the same elevation in the valley are selected, the Z-RMS of the check points increases to 45 cm (row “GK3: SM_7GCPs” in Table 7). While the residuals of the GCPs are otherwise large (and thus indicating the issues caused by the neglected scale distortion), they are absolutely unremarkable in this elevation-restricted variant.

This contribution has been peer-reviewed. The double-blind peer-review was conducted on the basis of the full paper.
https://doi.org/10.5194/isprs-annals-XI-2-2026-29-2026 | © Author(s) 2026. CC BY 4.0 License.

[cm]		GCPs (n=10) (*n=7)					check points (n=169) (*n=172)				
		min	mean	medi	MAX	**RMS**	min	mean	medi	MAX	**RMS**
GK3: nM	X	-2	4	5	13	**6**	-13	7	7	24	**9**
	Y	-4	9	11	21	**13**	-11	11	11	35	**15**
	Z	-64	21	16	14	**33**	-85	-32	-31	14	**40**
GK3: BM	X	1	13	12	27	**16**	-11	7	6	38	**11**
	Y	-6	6	5	18	**9**	-12	10	10	29	**13**
	Z	-39	1	8	35	**25**	-49	7	9	56	**26**
GK3: SM	X	-10	0	-1	16	**8**	-23	3	3	23	**8**
	Y	-12	0	-2	15	**9**	-20	3	3	31	**11**
	Z	-30	0	10	26	**21**	-48	6	9	41	**23**
GK3: (*) SM_7GCPs	X	-5	0	-1	7	**4**	-19	8	8	30	**12**
	Y	-5	0	0	9	**5**	-18	6	6	34	**13**
	Z	-8	0	2	4	**4**	-22	39	41	73	**45**

Table 7. Residuals of the terrain points after the AT with Orient in GK3 (*GIS-Grid*, *MGI heights*), but without considering scale distortion, estimating different mounting variants: nM (no mounting), BM (block mounting), SM (mounting per strip), SM_7GCPs (mounting per strip, but 7 GCPs in the valley only).

All previous results (with and without considering scale distortion) were obtained using the TU Wien software Orient. To compare these results with those from a commercial software, calculations were performed using Match-AT (part of ApplicationsMaster) by Trimble/Inpho (version 11.0.7). This version does not consider scale distortion. Unlike in Orient, the INS observations of the rotation angles are not used, because rotation misalignments in Match-AT cannot be determined separately for each strip (only once for the entire block). However, all tie points are used. The following variants are calculated with Match-AT:

• **An unknown 3D shift per strip.** This approach is expected to compensate for the average effect of scale distortion.

• **Shift-and-drift approach.** This method determines an unknown 3D shift per strip and additionally a linear change to it (i.e., a drift).

• **Adaption of the principal distance.** As described in (Ressl, 2002), the effect of scale distortion τ can be (fully) compensated in (exact) vertical images by modifying the principal distance from c to c_τ:

$$c_\tau = c/\tau \quad (1)$$

For smaller block extents, it is sufficient to determine a single new principal distance for all images in this manner, where τ is calculated at the block centre (problem P2 in Chapter 2). However, for larger blocks, the variation of τ from the western to the eastern border of the block must be considered (problem P3). In the present block, τ changes significantly from 28 ppm to 213 ppm (Figure 2). Therefore, the images are divided into five groups based on the easting coordinate of their projection centres, each group with its own new principal distance. The Inpho project then contains five cameras. A 3D shift per strip is also determined.

• **Adaption of Z_0.** Alternatively, the effect of scale distortion in (exact) vertical images over horizontal terrain can be compensated by modifying the height of the projection centre (Z_0) while considering the average terrain height (Z_t) as follows:

$$Z_{0,\tau} = Z_t + \tau\cdot(Z_0 - Z_t) \quad (2)$$

This method has the disadvantage of being valid only for horizontal terrain, but the advantage that block size (and thus Problem P3 in Chapter 2) is irrelevant, as Z_0 is corrected for each image according to the locally effective τ. A similar method is proposed in (Legat, 2006). A 3D shift per strip is also determined.

Table 8 shows the results obtained by these AT variants. It is evident that, in particular, the two solutions c_τ+SS and $Z_{0,\tau}$+SS (where τ is explicitly introduced by the user) come very close to the optimal check point RMS values; i.e., (8, 11, 11) [cm] of GK3 in Table 6 (last row). If the relatively simple shift-only (SS) and shift-and-drift (SD) methods are applied, then the Z-RMS roughly doubles.

[cm]		GCPs (n=10)					check points (n=169)				
		min	mean	medi	MAX	**RMS**	min	mean	medi	MAX	**RMS**
GK3: MAT11 SS	X	-14	0	2	11	**9**	-28	2	3	25	**10**
	Y	-14	0	3	11	**10**	-25	1	1	28	**11**
	Z	-37	0	10	33	**26**	-56	4	5	50	**27**
GK3: MAT11 SD	X	-10	0	-1	13	**6**	-24	0	1	25	**8**
	Y	-28	0	6	13	**12**	-24	2	1	33	**12**
	Z	-15	0	1	16	**11**	-65	7	9	53	**20**
GK3: MAT11 c_τ+SS	X	-14	0	0	12	**9**	-29	3	3	27	**10**
	Y	-15	0	3	13	**11**	-27	1	0	28	**11**
	Z	-9	0	0	10	**6**	-34	-1	-3	36	**14**
GK3: MAT11 $Z_{0,\tau}$+SS	X	-17	0	-1	17	**11**	-32	0	1	26	**10**
	Y	-15	0	3	14	**11**	-26	1	1	27	**11**
	Z	-7	0	-2	12	**6**	-35	-1	-4	31	**15**

Table 8. Residuals of the terrain points after the AT with MATCH-AT (version 11.0.7, thus without scale distortion) in GK3 (*GIS-Grid*, *MGI heights*) in different variants: SS (3D shifts per strip), SD (shift & drift), c_τ+SS (adapting τ in c and 3D shifts per strip), $Z_{0,\tau}$+SS (adapting τ in Z_0 and 3D shifts per strip).

After completing the evalAT project (in spring 2024), the version 15 of ApplicationsMaster was released in autumn 2024. According to the manual, this version corrects not only refraction and Earth curvature but also “map projection effects” (setting: *correction model precise*). Calculations were subsequently repeated using this version (Table 9).

The results using version 15 demonstrate that the *correction model precise* yields check point RMS values that are very close to those of the $Z_{0,\tau}$+SS variant in Version 11 (Table 8, last row).

[cm]		GCPs (n=10)					check points (n=169)				
		min	mean	medi	MAX	**RMS**	min	mean	medi	MAX	**RMS**
GK3: MAT15 3x3TPs	X	-16	-1	-4	18	**11**	-30	0	0	23	**10**
	Y	-14	-3	-3	12	**9**	-26	0	0	28	**11**
	Z	-13	-4	-5	8	**7**	-44	-8	-9	24	**16**
GK3: MAT15 allTPs	X	-18	-2	1	11	**11**	-33	0	-1	27	**10**
	Y	-20	-1	0	20	**13**	-31	-2	-2	24	**11**
	Z	-11	-3	-6	11	**7**	-43	-7	-8	29	**16**
GK3: MAT15 allTPs*	X	-20	-2	-1	12	**12**	-34	-1	0	26	**10**
	Y	-16	-1	-1	15	**11**	-27	-1	0	26	**11**
	Z	-8	-3	-5	8	**6**	-45	-7	-7	29	**15**

Table 9. Residuals of the terrain points after the AT with Match-AT (version 15.0.4, with setting *correction model precise* with EPSG 31255), in GK3 (*GIS-Grid*, *MGI heights*) in the different variants: 3x3TPs (the same set of reduced tie points as in Orient), allTPs (using all tie points), allTPs* (using all tie points and a geoid).

This contribution has been peer-reviewed. The double-blind peer-review was conducted on the basis of the full paper.
https://doi.org/10.5194/isprs-annals-XI-2-2026-29-2026 | © Author(s) 2026. CC BY 4.0 License.

Version 15 also allows a geoid to be defined during project setup (third row in Table 9). This likely enables corrections or calculations in ellipsoidal heights, which would not strictly correspond to calculations in the GK3 system (*GIS-Grid, MGI heights*). However, the effect of this geoid is marginal in this context.

Furthermore, it is evident that reducing the number of tie points from approximately 228,000 to 7,000 in Match-AT makes no significant difference, confirming that this reduction was also justified in the Orient investigations.

6. Conclusions

In the evalAT project, jointly conducted by BEV and TU Wien, the quality of aerotriangulation (AT) in the map projection was investigated using a GNSS-INS-supported aerial image block consisting of 4342 vertical images in 22 main- and 5 cross-strips (covering an alpine area with an elevation range of 586 m to 2003 m).

Fundamentally, the AT in the map projection achieves the same accuracies as an AT in an undistorted (tangential) system. For the 169 GNSS-measured check points provided by BEV, the RMS values for (X, Y, Z) in the tangential system are (7, 10, 11) cm. Given the ground pixel size of 20 cm and an estimated image measurement accuracy of 0.2 pixels, the full photogrammetric accuracy potential is not fully realized, suggesting small remaining systematic errors (likely in the GNSS check point measurements).

In the original Gauss-Krüger projection (i.e., with ellipsoidal heights and without the *GIS-Grid*), these values are (6, 10, 11) cm. The AT in the official system of the Austrian national survey, which results from the original Gauss-Krüger projection by applying the *GIS-* and *Height-Grid*, only slightly degrades these values to (8, 11, 11) cm.

To achieve such accuracies in the map projection, it is essential to account for Earth curvature and scale distortion. The latter of which contributes approximately two-thirds of the Earth curvature effect in this dataset. If the scale distortion is neglected, the Z-RMS deteriorates depending on the elevation distribution of the GCPs; from 11 cm to 23 cm (in the “favorable” case examined here) or even to 45 cm (in the “unfavorable” case where all control points are at the same valley elevation).

In AT software that does not consider scale distortion, the problem can be partially mitigated by adapting the heights of the projection centers or the principal distance before the AT, yielding RMS values of approximately (10, 11, 15) cm.

Future work should focus on the adverse effects of the *GIS-* and *Height-Grid*. Their impact shows greater variability in other areas of Austria than in the dataset examined (see Figures 4 and 5). Consequently, it can be assumed that in these areas with greater variability, the free exterior orientations will compensate for smaller portions of these grids than in the current dataset; thus degrading the results to a larger extent compared with a tangential solution. Another topic for further investigation is the correct handling of Earth curvature and scale distortion in the context of oblique imagery.

References

BEV, 2025a. Homepage of the division remote sensing at the BEV with description of the field of duties, https://www.bev.gv.at/en/Topics/Remote-Sensing.html, last access 2025.10.27.

BEV, 2025b. Description of the BEV product GIS-Grid, https://www.bev.gv.at/Services/Produkte/Grundlagenvermessung/GIS-Grid.html, last access 2025.10.27.

BEV, 2025c. Description of the BEV product Height-Grid plus Geoid, https://www.bev.gv.at/Services/Produkte/Grundlagenvermessung/Hoehen-Grid-plus-Geoid.html, last access 2025.10.27.

BEV, 2025d. Description of the BEV product Transformation Parameters, https://www.bev.gv.at/Services/Produkte/Grundlagenvermessung/Transformationsparameter.html, last access 2025.10.27.

Heipke, C., Jacobsen, K., Wegmann, H., Andersen, Ø. & Nilsen JR., B., 2002. Test goals and test set up for the OEEPE test „Integrated Sensor Orientation”. *OEEPE Official Publication No. 43 "Integrated Sensor Orientation Test Report and Workshop Proceedings"*, 11-18.

Jacobsen, K., 2002. Transformations And Computation Of Orientation Data In Different Coordinate Systems. *OEEPE Official Publication No. 43 "Integrated Sensor Orientation Test Report and Workshop Proceedings"*, 179-186.

Kager, H., 1989. ORIENT: A Universal Photogrammetric Adjustment System. *Optical 3-D Measurement Techniques*, Grün/Kahmen (editors), 447-455.

Legat, K., 2006. Approximate direct georeferencing in national coordinates. *ISPRS J. Photogram. Rem. Sens.* 60 (4), 239–255.

McGlone, J. C. (editor), 2013. *Manual of Photogrammetry, Sixth Edition*, ASPRS.

Ressl, C., 2002. The Impact of Conformal Map Projections on Direct Georeferencing. *ISPRS Archives*, Comm. III Symposium, Graz, 9 - 13 September 2002.

Ressl, C., Pfeifer, N., Ressl, C., Bayr, A., 2025. Das Projekt *evalAT* zur Untersuchung der Genauigkeit der Aerotriangulation im Landessystem. *Dreiländertagung der DGPF, der OVG und der SGPF in Muttenz, Schweiz – Publikationen der DGPF, Band 33*, 2025. DOI: 10.24407/KXP:1928486096.

Snyder, J. P., 1987. Map Projections – A Working Manual. *U.S. Geological Survey professional paper;*1395.

Wang, S., 1980. Einfluß der geodätischen Abbildungs-verzerrungen auf die photogrammetrische Punktbestimmung, Dissertation, Deutsche Geodätische Kommission, Reihe C, Nr. 263